Cerebral Cortex, August 2017;27: 3930–3942

doi: 10.1093/cercor/bhw206
Advance Access Publication Date: 8 July 2016
Original Article

ORIGINAL ARTICLE

Inhibition of Information Flow to the Default Mode Network During Self-Reference Versus Reference to Others

Joram Soch[1,2,3], Lorenz Deserno[2,4,5], Anne Assmann[1,5], Adriana Barman[1], Henrik Walter[2], Alan Richardson-Klavehn[5], and Björn H. Schott[1,2,5,6]

[1]Department of Behavioral Neurology, Leibniz Institute for Neurobiology, Magdeburg, Germany, [2]Department of Psychiatry and Psychotherapy, Campus Mitte, Charité – Universitätsmedizin, Berlin, Germany, [3]Bernstein Center for Computational Neuroscience, Berlin, Germany, [4]Max Planck Institute for Human Cognitive and Brain Sciences, Leipzig, Germany, [5]Department of Neurology, Otto von Guericke University, Magdeburg, Germany, and [6]Center for Behavioral Brain Sciences, Magdeburg, Germany

Address correspondence to Dr. Björn Schott, Leibniz-Institut für Neurobiologie, Brenneckestraße 6, 39118 Magdeburg, Germany. Email: bjoern.schott@med.ovgu.de

Abstract

The default mode network (DMN), a network centered around the cortical midline, shows deactivation during most cognitive tasks and pronounced resting-state connectivity, but is actively engaged in self-reference and social cognition. It is, however, yet unclear how information reaches the DMN during social cognitive processing. Here, we addressed this question using dynamic causal modeling (DCM) of functional magnetic resonance imaging (fMRI) data acquired during self-reference (SR) and reference to others (OR). Both conditions engaged the left inferior frontal gyrus (LIFG), most likely reflecting semantic processing. Within the DMN, self-reference preferentially elicited rostral anterior cingulate and ventromedial prefrontal cortex (rACC/vmPFC) activity, whereas OR engaged posterior cingulate and precuneus (PCC/PreCun). DCM revealed that the regulation of information flow to the DMN was primarily inhibitory. Most prominently, SR elicited inhibited information flow from the LIFG to the PCC/PreCun, while OR was associated with suppression of the connectivity from the LIFG to the rACC/vmPFC. These results suggest that task-related DMN activation is enabled by inhibitory down-regulation of task-irrelevant information flow when switching from rest to stimulus-specific processing.

Key words: default mode network, dynamic causal modeling, effective connectivity, self-reference, social cognition

Introduction

The complexity of human social interactions is largely unparalleled in the animal kingdom. Such complex social interactions require an individual to engage in a variety of cognitive tasks, with the distinction between oneself and others constituting a fundamental basis of human social cognition (Moran et al. 2013). At a neural level, social cognition engages a network centered around cortical midline structures including the rostral anterior cingulate and ventromedial prefrontal cortex (rACC/vmPFC), the posterior cingulate cortex and precuneus (PCC/PreCun), and the temporo–parietal junction (TPJ) (Kelley et al. 2002; Fossati et al. 2003; Sajonz et al. 2010; Qin and Northoff 2011). Social cognitive tasks that engage this network include self-reference (SR) and reference to others (OR) (Kelley et al. 2002; Macrae et al. 2004; Moran et al. 2006; Qin et al. 2012), mentalizing and Theory of Mind (Spreng et al. 2009; Schnell et al.

2011), or episodic memory retrieval (Fink et al. 1996; Schott et al. 2005; Sajonz et al. 2010). A rather unique feature of this cortical network is its propensity to show increased activations during conditions of relative rest compared to the conditions of cognitive tasks like attention or working memory. More generally, it exhibits higher activation during relatively easy compared to more cognitively demanding conditions in functional neuroimaging studies. It is therefore commonly referred to as the Default Mode Network (DMN) (Gusnard et al. 2001; Raichle et al. 2001; Schilbach et al. 2012). The DMN exhibits strong intrinsic functional connectivity during the resting state (Beckmann et al. 2005; Fox et al. 2005), and several authors have pointed out the remarkable overlap of the resting-state DMN with the neural signatures of social cognition in task-based functional magnetic resonance imaging (fMRI) (Gusnard et al. 2001; Mars et al. 2012; Schilbach et al. 2012). An influential interpretation of the striking similarity between brain activity patterns related to resting conditions and those elicited by social cognitive tasks is the hypothesis that DMN activity at "rest" may reflect spontaneous self-related or social-cognitive processing or spontaneous autobiographical retrieval ("mind-wandering") (Gusnard et al. 2001; Buckner et al. 2008; Schilbach et al. 2012; Fox et al. 2015).

When engaged in social cognitive tasks, DMN structures show a certain degree of functional specialization (Salomon et al. 2014) that is also evident in distinct patterns of structural connectivity (Zhang et al. 2014). A well-known example of functional specialization within the DMN is the well-replicated finding that the rACC/vmPFC is preferentially involved in self-referential relative to other-referential processing (Kelley et al. 2002; Moran et al. 2013) and also relative to episodic memory retrieval (Sajonz et al. 2010; Qin et al. 2012). The specific involvement of the rACC/vmPFC in SR has been confirmed by 2 meta-analyses (Qin and Northoff 2011; Denny et al. 2012), which have further suggested that posterior midline structures, namely the PCC/PreCun (Qin and Northoff 2011) and the adjacent cuneus (Denny et al. 2012), might preferentially process information related to others rather than oneself.

Given the lack of directly stimulus-responsive brain structures within the DMN, the regionally specific involvement of DMN structures in SR and social cognition cannot be readily explained without considering the influx of semantic information into DMN structures. This raises the question how the specific engagement of the DMN in different tasks, such as SR versus OR, is controlled, and, more generally, how the flow of external information to DMN subregions is regulated. In order to address this question, measures of effective, that is, directional connectivity between brain structures such as dynamic causal modeling (DCM) are required. Previous studies have applied measures of effective connectivity to the DMN at rest using Granger causality (Jiao et al. 2011) and stochastic DCM (Li et al. 2012; Di and Biswal 2014; Bastos-Leite et al. 2015). Those studies have identified the PCC/PreCun and – to a somewhat lesser extent – the rACC/vmPFC as hub regions of the DMN that receive input from other DMN structures like the TPJ (Jiao et al. 2011; Di and Biswal 2014). Results regarding the intrinsic connectivity of the midline structures are not entirely conclusive yet. Di and Biswal (2014) found the rACC/vmPFC and the PCC/PreCun to be mutually and positively connected, whereas Di and Biswal (2014) reported rather sparse effective connectivity that was limited to the rACC/vmPFC → PCC/PreCun connection, but not significant in the opposite direction. Those apparently conflicting results may be explained by modulatory influences on intrinsic DMN connectivity. In line with this notion, a comparative investigation of DMN effective connectivity during rest relative to task-induced deactivation has revealed increased within-DMN connectivity during the task conditions, possibly reflecting decreased regional specialization during relative deactivation (Li et al. 2012).

While those studies have provided important insight into the intrinsic effective connectivity of the DMN, they could not provide information on the information flow to DMN subregions during social cognitive tasks. The main reason for this is that resting-state or rest-task comparisons typically elicit relatively isolated activation of the DMN. Instead, to investigate the information flow to the DMN during social cognition, it may be more suitable to employ task-based fMRI acquired during social cognitive tasks that engage not only the DMN, but also brain regions involved in semantic evaluation of stimuli. One brain region that commonly co-activates with the DMN during self-referential processing is the left inferior frontal gyrus (LIFG; Brodmann Area, BA 45/47) (Morin and Michaud 2007). The LIFG overlaps, at least in part, with Broca's language area, and has been implicated in semantic analysis of verbal information (Demb et al. 1995; Poldrack et al. 1999; Martins et al. 2014). Compatible with the notion that the LIFG may process information semantically before self-referential or social evaluation can occur, a meta-analysis has implicated LIFG activation in evaluative or semantic rather than perceptual SR (Morin and Michaud 2007). Moreover, social or self-referential encoding tasks have yielded comparable levels of LIFG activation during SR and verbal semantic control tasks like OR or social desirability rating compared to non-semantic control tasks (Craik et al. 1999; Kelley et al. 2002).

In the present study, we applied bilinear, deterministic DCM in conjunction with Bayesian model selection (BMS) and averaging (BMA) (Penny et al. 2004; Stephan et al. 2009) to event-related fMRI data acquired from 110 young healthy participants during the performance of a SR task (Kelley et al. 2002; Schott et al. 2014). In that task, participants were presented with adjectives describing personality traits and were asked to judge whether the adjective applied to themselves (SR), whether it applied to a famous person, the German chancellor Angela Merkel (OR), or whether it had exactly 2 syllables (non-semantic control condition). Compatible with previous findings, General Linear Model (GLM)-based fMRI data analysis revealed increased rACC/vmPFC activation during self-referential processing and preferential engagement of the PCC/PreCun during OR (Qin and Northoff 2011) as well as increased LIFG activation during the social semantic tasks compared to the non-semantic control task (syllable counting) (Schott et al. 2013). DCM was then employed to assess how the specific activation of the rACC/vmPFC during SR and the preferential engagement of the PCC/PreCun during other-reference was controlled at a network level. Under the assumption that external information needs to be processed semantically before undergoing further processing within the DMN, we chose the LIFG as input region. We hypothesized that activation differences between SR versus OR in the DMN core regions rACC/vmPFC and PCC/PreCun might originate from excitatory modulation of projections from the LIFG into the DMN and additional reciprocal inhibition of connections within the DMN.

Materials and Methods

Participants

In total, 110 neurologically and psychiatrically healthy young adults (53 male, 57 female, all right-handed, age range 19–31

years, mean age 24.37 ± 2.397 years) participated in the experiment. This study was approved by the Ethics Committee of the Medical Faculty of the Otto von Guericke University in Magdeburg, Germany, and was conducted in accordance with applicable ethical guidelines such as the Declaration of Helsinki.

Stimuli

For the purpose of this paradigm, a list of 330 words was generated as a basic database using the reloaded Berlin Affective Word List (BAWL-R) (Vo et al. 2009) and a study investigating age-dependent word rating on various scales (Gruhn and Smith 2008) as sources. Twenty six volunteers who did not participate in the actual study performed an emotional responsiveness rating, rating each word using values between 1 and 6. Based on the average rating, the 126 most positive and the 126 most negative words were compiled into 2 word lists that together contained the 252 most non-neutral words. For each participant, 168 words were randomly assigned to the experimental conditions so that 28 positive and 28 negative words were shown in each of the 3 conditions. The assignment was based on the anonymous subject code assigned to each subject by the fMRI laboratory of the Department of Neurology at the University of Magdeburg (e.g., "aa12", "xy99"). The remaining one-third of the 252 words was used for a surprise memory test after the fMRI paradigm. Stimulus delivery and experimental control were performed using the software Presentation (Neurobehavioral Systems). During the fMRI experiment, the PC was synchronized with the MRI scanner to ensure trouble-free presentation and jittering.

Paradigm

The participants performed a version of the well-established self-referential processing task (Craik et al. 1999; Kelley et al. 2002) that was optimized for DCM by employing a single fMRI run and a near-exponential jitter to improve the estimation of the trial-specific BOLD responses at single-subject level (Hinrichs et al. 2000).

Subjects were presented with adjectives describing desirable and undesirable personality traits and were asked to either judge whether the personality trait applied to themselves (SR), whether it applied to a famous person (the Federal Chancellor of Germany, Angela Merkel) (OR) or whether the adjective had 2 syllables or not (syllable counting, SC), depending on the cue word presented along with the adjective (Supplementary Fig. S1). The syllable counting task was chosen as baseline condition because it requires little semantic processing, but comparable phonological processing as the tasks of interest (Richardson-Klavehn and Gardiner 1998; Schott et al. 2002, 2013). Participants responded by pressing the left or right button using the index and middle finger of their right hand, depending on their decision.

Subjects were requested to respond before the next word was shown and just focus their attention on the next word, if they had missed a response before the start of the next trial. All trials lasted 2500 ms and were followed by variable, near-exponentially distributed inter-trial-intervals between 1500 and 9500 ms, using a plus sign as central fixation. All cues and stimuli were shown in German language. The paradigm lasted 16:20 min with 16:40 min of fMRI scanning.

MRI Data Acquisition

fMRI was performed on a GE Signa Horizon LX, a 1.5 T MR tomograph (General Electric Healthcare) on the Medical Campus in Magdeburg. First, a sagittal T1-weighted image was recorded in order to align slices in parallel to the line from anterior commissure (AC) to posterior commissure (PC). Next, a proton density weighted image (PD image) was acquired (70 slices, 256 × 256 in-plane resolution, voxel size = 0.8 × 0.8 × 2 mm). The PD image was later used as an anatomical reference for spatial co-registration and optimized spatial normalization.

fMRI data consisted of 500 T2*-weighted echo-planar images (TR = 2 s, TE = 35 ms, flip-α = 80°; 23 slices, 64 × 64 in-plane resolution, voxel size = 3.1 × 3.1 × 5 mm (4 mm + 1 mm gap)) acquired in a bottom-to-top interleaved fashion with odd images first. Prior to actual data acquisition, 6 EPIs were recorded and discarded from data analysis to allow for steady-state magnetization at the beginning of a functional run.

fMRI Data Preprocessing

Data preprocessing and analysis were performed using Statistical Parametric Mapping (SPM8; Wellcome Trust Center for Neuroimaging, University College London, London, UK). EPIs were corrected for acquisition time delay (slice timing) and head-motion (realignment). Then, the anatomical scan was co-registered to the mean functional image and segmented into tissue types. The resulting parameters were used to normalize scans into the MNI space using a voxel size of 3 × 3 × 3 mm. Finally, the images were spatially smoothed using a Gaussian kernel with an FWHM of 8 mm.

GLM-Based Analyses

Functional neuroanatomy of SR versus OR was assessed using 2-stage mixed-effects statistics based on GLM as implemented in SPM.

At the first stage, single subjects' hemodynamic response was modeled by convolving box-car functions at stimulus presentation with a canonical hemodynamic response function (HRF). The resulting time courses were sampled down for each scan to form covariates of a GLM. The GLM included separate covariates for each condition of interest (SR, OR, SC), parametric modulators describing the subject's response (+ 1 or – 1), the 6 movement parameters determined from spatial realignment as covariates of no interest, and a constant regressor representing the implicit baseline. Model estimation was performed using a restricted maximum likelihood (ReML) fit. In previous studies using the task employed here (Macrae et al. 2004), trials of each condition were usually divided into 2 categories based on the subject's response. In the present GLM, all trials from one condition enter one regressor, thus providing better estimates for task-related neural activity, in which we were primarily interested, while still allowing to capture response-related neural activity using parametric modulation.

At the second level, experimental conditions were tested against each other using a one-way 3-level random effects ANOVA (using condition as one factor with 3 levels). Statistical inference was performed using a significance threshold of $p = 0.05$, FWE-corrected for multiple comparisons at the whole brain with an extent threshold of $k = 10$ adjacent voxels. Statistical tests addressed 3 contrasts of interest: positive effects of both experimental conditions against the control condition ("both > base"), effects of SR against OR ("self > other") and vice versa ("other > self").

Dynamic Causal Modeling

Overview

DCM was performed using DCM10 as implemented in SPM8. DCM is a Bayesian network modeling approach that provides estimates of effective connectivity as well as its extrinsic modulation by experimental conditions (Friston et al., 2003; Stephan et al. 2008). The neural model includes parameters for

1. regional activation evoked by experimental conditions ("extrinsic inputs"),
2. context-independent couplings between 2 regions ("intrinsic connections"), and
3. context-dependent influences of experimental conditions on intrinsic connections ("contextual modulations").

Here, we applied bilinear, deterministic, single-state DCMs for fMRI with mean-centered inputs.

Network Nodes and Regions of Interest

Regions of interest (ROIs) were defined using a combination of functional and anatomical criteria: At the group level, thresholded statistical parametric maps (SPMs) were masked with anatomical constraints taken from Automated Anatomical Labeling (AAL), a canonical parcellation of the human brain (Tzourio-Mazoyer et al. 2002). Based on the prominent role of the DMN in social cognition and particularly self-referential information processing (Qin and Northoff 2011) and guided by previous studies implicating the LIFG in deep (i.e., semantic) processing of verbal information, the following brain structures structures were chosen as nodes of interest:

1. The complex formed by rACC/vmPFC has repeatedly been shown to preferentially process self-referential information (Qin and Northoff 2011; Denny et al. 2012), a finding replicated in the present study (Fig. 1*B*). The ROI for rACC/vmPFC was defined by multiplying the T-contrast *"positive effects of self-reference"* (self > other) with the anatomical boundaries of orbitomedial frontal gyrus and anterior cingulate gyrus from the AAL atlas.
2. The complex formed by the PCC/PreCun has been demonstrated to preferentially activate during OR rather than SR (Qin and Northoff 2011), which we were also able to confirm (Fig. 1*B*). We thus multiplied the T-contrast *"positive effects of reference to others"* (other > self) with the precuneus and posterior cingulate gyrus AAL masks to obtain a ROI for PCC/PreCun.
3. The LIFG, encompassing Broca's language area and adjacent portions of Brodmann areas (BA) 45 and 47, was used as the network's driving input region given its role in semantic processing (Demb et al. 1995; Poldrack et al. 1999; Schott et al. 2013). We observed LIFG activation at comparable levels during both SR and OR relative to the syllable counting condition (Fig. 1A), suggesting that it reflected semantic evaluation of the word stimuli (Morin and Michaud 2007) or levels of processing (Schott et al. 2013). Given the close proximity of the LIFG and the anterior insula – a landmark structure of the salience network (Goulden et al. 2014; Kucyi and Davis 2014) – we had to restrict our ROI to portions of the activation cluster that were actually located within the LIFG. Therefore, the T-contrast *"positive effects of social processing"* (self + other > 2 × syllables) was multiplied with the AAL mask of the LIFG, yielding a ROI for the LIFG.

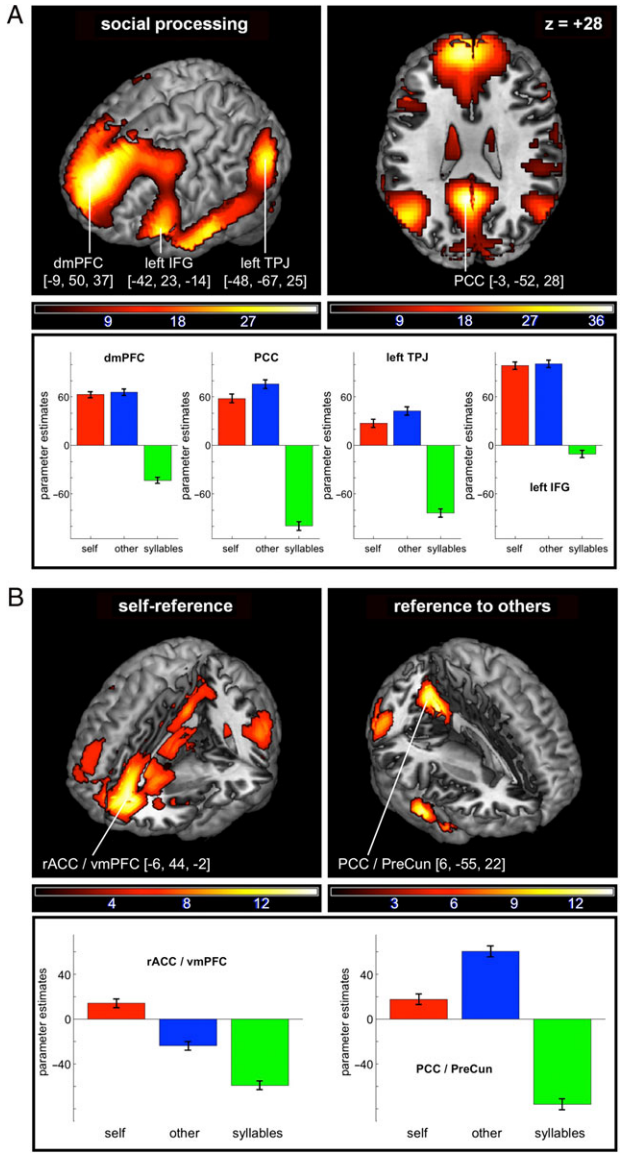

Figure 1. GLM results. Activation maps display test statistics from second level analysis. Bar plots show contrast estimates at peak voxels in brain structures linked to self-referential and other-referential processing. (*A*) Positive effects of social processing (SR+OR > base). Left panel: lateral view displaying dorsomedial prefrontal cortex (dmPFC), left IFG and left TPJ. Right panel: axial section at z = 28 mm. (*B*) Direct comparison of SR and OR (SR > OR and OR > SR). Left panel: The rACC/vmPFC shows increased activation during SR. Right panel: The PCC/PreCun is relatively more active during OR.

Within the resulting ROIs (Supplementary Fig. S2), spheres (r = 6 mm) were seeded around the peak voxels of the respective contrasts of interest, separately for each subject, to improve signal-to-noise ratio. The first eigenvariate time series were extracted from the resulting volumes of interest (VOIs) and adjusted for effects of interest, as modeled and explained by the individual first-level GLMs.

Model Space

The aim of our DCM analyses was to elucidate the differential activation patterns within the DMN during self-referential versus other-referential processing. Because previous DCM studies of the DMN have reported mixed results with respect to

intrinsic DMN effective connectivity during rest (Di and Biswal 2014; Sharaev et al. 2016) and because none of those studies had included the IFG, we employed a 2-step approach. We first set up a model space with no contextual modulations in order to investigate the intrinsic connections within the 3-region network defined above. This initial step was performed for both the left IFG and right IFG. In a second step, the model space was expanded by including contextual modulations on the existing connections in the models. Because BMS at the first step did not support the assumption of full intrinsic connectivity in the network that included the right IFG (Fig. 2), the second step was only performed on the network encompassing the left IFG (Fig. 3).

With social processing of any type (SR as well as OR) requiring semantic analysis of the processed information, the LIFG was assumed to act as an input region, since it may be considered a first processing station in which semantic analysis of verbal stimuli takes place (Demb et al. 1995; Poldrack et al. 1999; Schott et al. 2013). Therefore, all SR and OR trials served as an extrinsic input into this region. Furthermore, only intrinsic connections leading from LIFG to midline regions (i.e., LIFG → rACC/vmPFC and LIFG → PCC/PreCun) were included in all models, because we assumed that information flow from this brain structure involved in semantic processing to the DMN would be a prerequisite for any further information processing within the DMN. All other connections (rACC/vmPFC → LIFG, PCC/PreCun → LIFG, rACC/vmPFC → PCC/PreCun, PCC/PreCun → rACC/vmPFC) were either included or not, leading to $2^4 = 16$ DCMs. When performing Bayesian model selection (see below) in this model space, we found the model with all intrinsic connections to be clearly superior (Fig. 2A). As a control, the same approach was applied to the right instead of the left IFG, yielding evidence for a sparse intrinsic connectivity pattern(Fig. 2B).

Therefore, the analysis of contextual modulations was performed on the network including left IFG only, and full intrinsic connectivity of the 3 regions was assumed from here on.

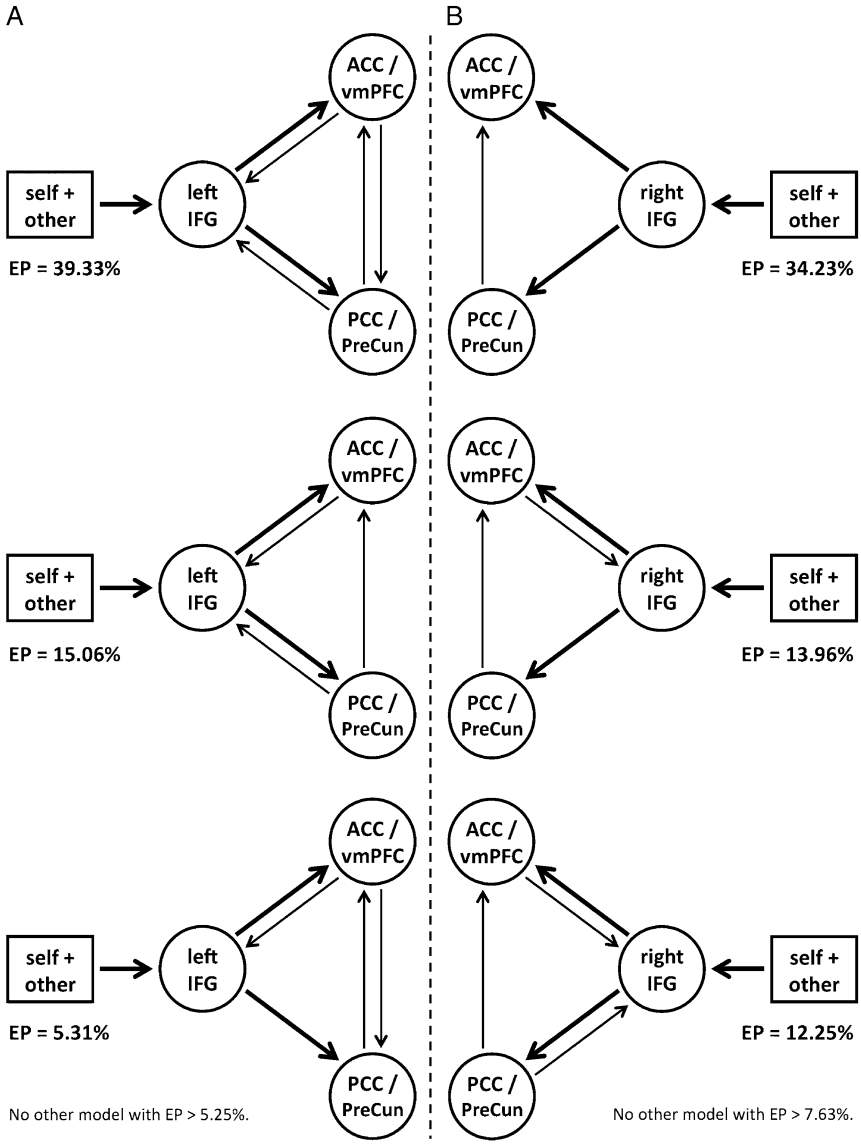

Figure 2. DCM preanalysis: intrinsic connections. The preliminary BMS on DCMs without contextual modulations was performed on the connections of the rACC/vmPFC and PCC/PreCun with the left and right IFG, separately. (A) Left IFG intrinsic connections. As depicted in the top row, the winning model included full intrinsic connectivity. (B) Right IFG intrinsic connections. A different connectivity pattern was observed in the right hemisphere, allowing no definite assumptions with respect to intrinsic connectivity.

Variable features in the network structure were then established by contextual modulations that differed across models. Each connection leading to the rACC/vmPFC (i.e., LIFG → rACC/vmPFC and PCC/PreCun → rACC/vmPFC) or to the PCC/PreCun (i.e., LIFG → PCC/PreCun and rACC/vmPFC → PCC/PreCun) was allowed to be modulated by both SR and OR in order to account for potential excitatory and inhibitory effects. This yielded 2^8 = 256 DCMs (Fig. 3A). From this set, models assuming no modulation by at least one of the 2 conditions were discarded, because both experimental conditions were hypothesized to influence DMN effective connectivity during social cognitive processing, resulting in the final model space of 256–31 = 225 DCMs (Supplementary Fig. S3).

Model Selection and Parameter Inference

BMA and BMS were performed using DCM10 as implemented in SPM8. BMS searches the model space for the model that best balances model accuracy (as quantified by the probability of the data given the parameters) and complexity (as quantified by the distance between parameter priors and posteriors) using data from a group of subjects (Penny et al. 2004; Stephan et al. 2009). BMS uses the log model evidence as a measure of model quality. Here, random-effects Bayesian model selection (RFX BMS) was performed, meaning that network architecture and model structure were not assumed to be constant (i.e., not fixed) across subjects. RFX BMS was performed across 225 models from 110 subjects.

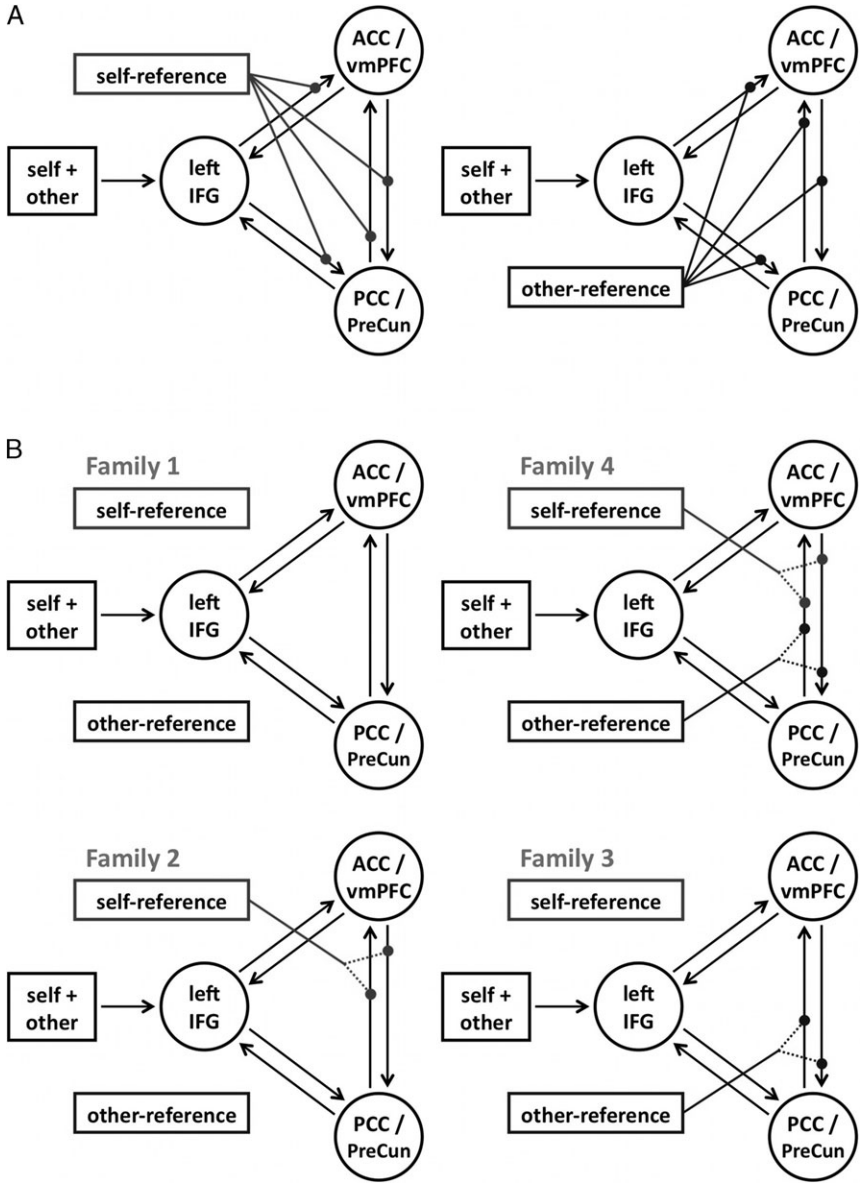

Figure 3. DCM methods: model space. DCM analyses used a 3-region network consisting of LIFG, rACC/vmPFC, and PCC/PreCun. In each model, LIFG receives driving input in all SR and OR trials. Furthermore, LIFG is fully connected intrinsically to rACC/vmPFC and PCC/PreCun, which are also connected reciprocally. (*A*) Contextual modulations defining the model space. Each connection leading to rACC/vmPFC or PCC/PreCun could be potentially modulated by SR and/or OR. Models without any contextual modulation by one of the experimental conditions were excluded from the model space, resulting in 15 "SR models" (left panel) and 15 "OR models" (right panel), which gave rise to 225 DCMs (Supplementary Fig. S2). (*B*) Family division of the model space. DCMs were grouped into 4 families (arranged counter-clock-wise) consisting of models with intra-DMN modulations by SR (Family 2), models with intra-DMN modulations by OR (Family 3), models with both modulations (Family 4) and models with none of these modulations (Family 1).

Table 1 Parameter estimates from Bayesian model averaging

Parameter	Estimates	T-value	p-value
Extrinsic input into the network			
self + other into left IFG	0.590 ± 0.208	29.83	<0.0028**
Intrinsic connections within regions			
left IFG→left IFG	−0.802 ± 0.122	−68.83	<0.0028**
rACC/vmPFC→rACC/vmPFC	−0.822 ± 0.128	−67.19	<0.0028**
PCC/PreCun→PCC/PreCun	−0.866 ± 0.122	−74.74	<0.0028**
Intrinsic connections between regions			
left IFG→rACC/vmPFC	0.240 ± 0.256	9.85	<0.0028**
left IFG→PCC/PreCun	0.409 ± 0.329	13.01	<0.0028**
rACC/vmPFC→left IFG	0.057 ± 0.259	2.31	0.023*
PCC/PreCun→left IFG	0.087 ± 0.305	3.01	0.003*
rACC/vmPFC→PCC/PreCun	−0.223 ± 0.294	−7.95	<0.0028**
PCC/PreCun→rACC/vmPFC	0.010 ± 0.237	0.44	0.661
Contextual modulations by experimental conditions			
SR on left IFG → rACC/vmPFC	0.036 ± 0.130	2.86	0.005*
SR on left IFG → PCC/PreCun	−0.514 ± 0.798	−6.75	<0.0028**
SR on rACC/vmPFC → PCC/PreCun	−0.018 ± 0.435	−0.42	0.672
SR on PCC/PreCun → rACC/vmPFC	−0.021 ± 0.498	−0.44	0.658
OR on left IFG → rACC/vmPFC	−1.481 ± 0.710	−21.88	<0.0028**
OR on left IFG → PCC/PreCun	0.000 ± 0.056	0.07	0.940
OR on rACC/vmPFC → PCC/PreCun	−0.427 ± 0.865	−5.17	<0.0028**
OR on PCC/PreCun → rACC/vmPFC	0.026 ± 0.290	0.95	0.346

Connectivity estimates and their standard deviations are given for the averaged model parameters obtained from Bayesian model averaging (Fig. 5B). *T* and *p* values refer to one-sample *t*-tests using an uncorrected threshold of $p = 0.05$ (*) and a Bonferroni-corrected threshold of $p = 0.0028$ (**).

The best fitting model was chosen based on so-called exceedance probabilities (EP), the probability for each model of being the most frequent in the population investigated. Recently, protected exceedance probabilities (PEPs) have been suggested to provide a more robust group-level measure in BMS, as they account for the possibility that differences in model frequencies occur by chance (Rigoux et al. 2014). Therefore, we also computed PEPs as implemented in spm_BMS contained in SPM12. Furthermore, a family selection was performed to address the question whether or not the self-other distinction might arise from contextual modulation between the DMN midline structures. To this end, we divided the model space into 4 model families (Fig. 3B) consisting of

1. models with no modulation of within-DMN connections ("Family 1", 9 models),
2. models with modulation of rACC/vmPFC ↔ PCC/PreCun connections by SR ("Family 2", 36 models),
3. models with modulation of rACC/vmPFC ↔ PCC/PreCun connections by OR ("Family 3", 36 models), and
4. models allowing for both types of modulations ("Family 4", 144 models).

Following model family selection, we performed BMA in the winning model families. BMA provides averaged parameter estimates accounting for the uncertainty over models as approximated by the log model evidences. These averaged parameters were tested using one-sample *t*-tests with a significance level of p = 0.05 and a Bonferroni-corrected threshold of $p = 0.0028$ (Table 1). Furthermore, DCM parameter estimates of the individual winning model and of the second-ranking model were tested using one-sample *t*-tests with a significance level of $p = 0.05$ and Bonferroni-corrected thresholds of $p = 0.0042$ (Supplementary Table S4) and $p = 0.0038$ (Supplementary Table S5).

Results

Regionally Specific DMN Activations

We first conducted a GLM-based analysis of our fMRI data to verify that brain regions previously linked to self-referential versus other-referential processing were reliably activated during task performance and to identify individual subjects' local maxima of activation within the brain regions of interest (LIFG, rACC/vmPFC, PCC/PreCun).

Irrespective of the specific condition (SR vs. OR), social processing relative to the non-semantic control condition (syllable counting) elicited activations in networks involved in semantic processing and in DMN structures (Fig. 1A). Prominent activations were observed in the ventrolateral prefrontal cortex, particularly the LIFG, most likely reflecting semantic processing (Demb et al. 1995; Poldrack et al. 1999; Schott et al. 2013; Martins et al. 2014). We also observed an activation of the right IFG during social processing, and a direct comparison of left and right IFG activation (averaged across all significant voxels within the AAL mask of the IFG) revealed that right IFG activation was significantly lower than left IFG activation ($F_{1.5,164.7} = 25.93$, $p < 0.001$; 2-way ANOVA for repeated measures with task (SR vs. OR vs. syllables) and hemisphere (left vs. right) as within-subject factors, Greenhouse–Geisser correction for non-sphericity applied). Both social judgment conditions also extensively engaged DMN structures like the dorsomedial prefrontal cortex, the PCC/PreCun, and the TPJ (Fig. 1A and Supplementary Table S3), most likely reflecting social cognitive processes (Qin and Northoff 2011; Denny et al. 2012; Schilbach et al. 2012).

While activations of the dorsomedial PFC were observed during both social cognitive tasks at comparable levels, more ventral parts of the anterior DMN (i.e., the rACC/vmPFC) showed a specifically more pronounced activation to SR when

compared to OR (Fig. 1B). Conversely, OR elicited a preferential activation in the posterior cingulate cortex and inferior portions of the precuneus (PCC/PreCun) (Fig. 1B). Supplementary Table S3 summarizes further fMRI activation differences related to self-referential relative to other-referential processing.

Intrinsic Effective Connectivity

In the first part of our analysis, we applied BMS to the DCMs of intrinsic connections, separately for the left and right hemisphere (Fig. 2). In the left hemisphere, the winning model suggested full intrinsic connectivity within the DMN and between the left IFG and both the rACC/vmPFC and the PCC/PreCun (Fig. 2A). In the right hemisphere, on the other hand, the winning model (and also the second-ranking model) suggested only sparse intrinsic connectivity within the network tested (EP of full intrinsic connectivity < 7.63%; see Fig. 2B). Therefore, DCM analyses of contextual modulations were performed in the left hemisphere only.

Effective Connectivity During SR Versus OR

Model Family Selection

DCMs were classified into model families based on whether within-DMN connections were modulated by SR (Family 2), OR (Family 3), both (Family 4) or none (Family 1). Model family selection (Fig. 4) strongly favored the model family with no within-DMN contextual modulation by SR or other-reference (Family 1, exceedance probability (EP) = 58.06%, protected exceedance probability (PEP) = 62.36%). The model family with contextual modulation of within-DMN connections by both SR and OR ranked second (Family 4, EP = 33.85%, PEP = 31.44%), and there was little support for the other model families (Family 2, EP = 1.80%, PEP = 0.38%; Family 3, EP = 6.29%, PEP = 5.82%).

Bayesian Model Averaging

Across the 2 winning families (1 and 4), BMA (Table 1, Fig. 5B) revealed significant intrinsic connections (except for PCC/PreCun → rACC/vmPFC). Regarding contextual modulations, we observed a significant negative modulation of the LIFG → PCC/PreCun connection by SR, whereas OR exerted an inhibitory influence on the LIFG → rACC/vmPFC and on the rACC/vmPFC → PCC/PreCun connections. The only significant positive modulation was observed on the LIFG → rACC/vmPFC during SR, but this modulation did not remain significant after Bonferroni correction.

Individual Model Selection

At the level of single models, BMS identified one model from Family 1 (Fig. 5C) that clearly outperformed all other 224 models tested with an exceedance probability of 67.76% (PEP = 55.81%). In this model, SR modulated the connection from the LIFG to the PCC/PreCun, while OR exerted its influence on the connection from the LIFG to the rACC/vmPFC. With an exceedance probability of 21.67% (PEP = 24.04%), a model from Family 4 ranked second (Fig. 5D). In that model, OR modulated the information flow from the LIFG to the rACC/vmPFC and from the rACC/vmPFC to the PCC/PreCun, whereas SR selectively influenced the information flow from the PCC/PreCun to the rACC/vmPFC. No other model exceeded a probability of 2.5%.

Parameter Inference

In the winning and in the second-ranking model (Fig. 5C and D), parameters of all auto-associative intrinsic connections and of extrinsic network inputs differed significantly from zero, with driving inputs being significantly positive (Supplementary Tables S4 and S5). Between-region intrinsic connections from the LIFG to both rACC/vmPFC and PCC/PreCun were also significantly positive in both models. In the winning model, contextual modulations of these connections by SR and other-reference were both significantly negative, indicating that SR exerted an inhibitory influence on the information flow from the LIFG to PCC/PreCun, the region preferably activated by other-reference; conversely, other-reference was associated with inhibitory influence on the information flow from the LIFG to rACC/vmPFC, the DMN subregion linked to SR. In the second-ranking model, OR exerted significant negative modulatory influence on

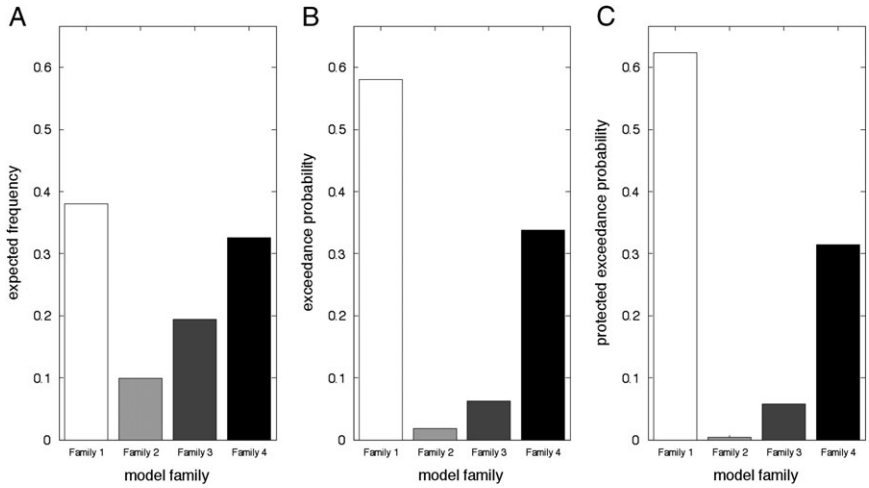

Figure 4. DCM results: model family selection. Model labels correspond to the family division of the model space (Fig. 3B). (*A*) Expected frequencies, (*B*) exceedance probabilities and (*C*) protected exceedance probabilities are reported as a measure of relative model quality. Bayesian model selection favored the model family without intra-DMN modulation (Family 1), followed by models with contextual modulations by both conditions (Family 4), while there was little evidence for models with intra-DMN modulation by only one condition (Families 2 and 3).

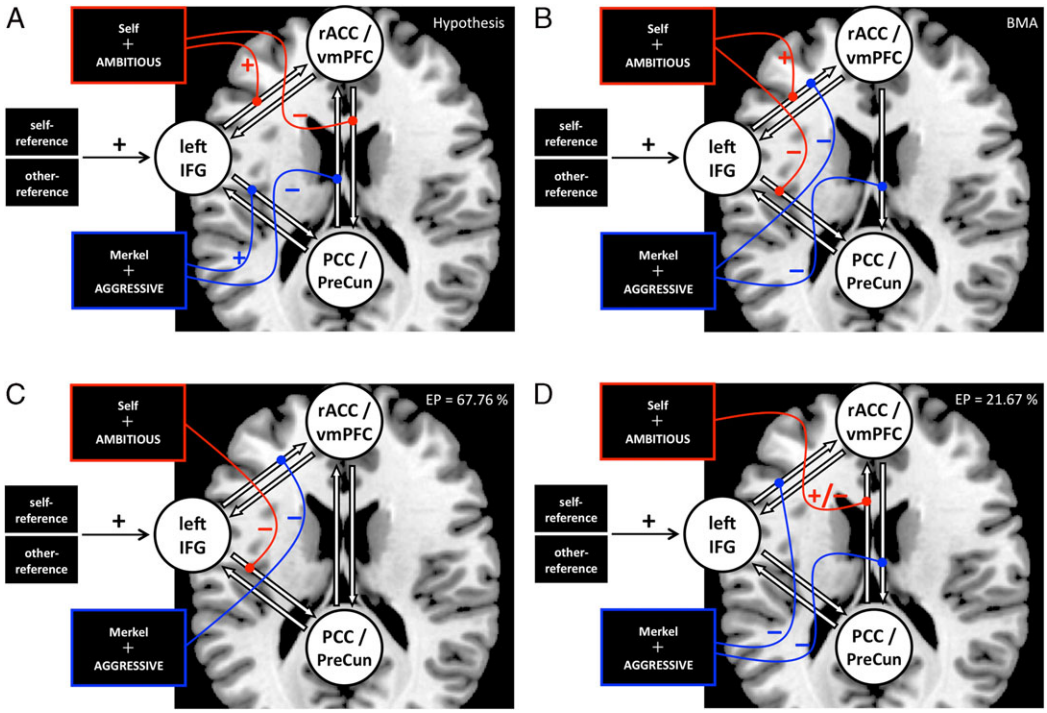

Figure 5. DCM results: model averaging and individual model selection. (*A*) Hypothesis: We had hypothesized independent excitation of connections from the LIFG to the DMN subregions by SR and OR, along with a potential inhibition of within-DMN connections. (*B*) Bayesian model averaging: Averaged model parameters significant at the group level largely reflect the winning model (*C*) and second-ranking model (*D*). One intrinsic connection (PCC/PreCun → rACC/vmPFC) was not significant at $p < 0.05$, despite full intrinsic connectivity in the winning and second-ranking models (*C*, *D*). One contextual modulation (SR on LIFG → rACC/vmPFC) stated in our initial hypothesis (*A*) was significant at $p < 0.05$, but not after Bonferroni correction. (*C*) Winning model: BMS favored a scenario of independent and mutual inhibition in which SR and OR negatively modulate connections leading to regions carrying the opposite experimental effects. (*D*) Second-ranking model: In this model, OR exerted inhibitory influence on both LIFG to rACC/vmPFC and PCC/PreCun to rACC/vmPFC connections. The model also included an influence of SR on the connection from PCC/PreCun to rACC/vmPFC, although the sign and significance of this modulation was not conclusively determined at the group level. No other model reached an exceedance probability of larger than 2.5%. Exceedance probabilities are reported as a measure of relative model quality. "–" and "+" refer to significant signed model parameters, whereas "+/–" refers to non-significant model parameters with no robust information with respect to sign.

the information flow from the LIFG to the rACC/vmPFC and from the rACC/vmPFC to the PCC/PreCun. While the model included a modulatory influence of SR on connectivity from PCC/PreCun to rACC/vmPFC, parameter inference did not yield conclusive information about the excitatory versus inhibitory nature of this modulation. On average, the parameter value was marginally negative (mean = –0.104), but the absolute coefficient of variation (CV) was substantially larger than one (|CV| = 9.902), suggesting that the modulation might be positive in some participants, but negative in others.

Discussion

In the present study, we aimed to elucidate how information flow to the DMN is regulated when anterior versus posterior DMN nodes are engaged in task-specific processing of self-referential versus other-referential information. In our GLM-based fMRI analysis, we replicated the previously described specialization of DMN subregions with the rACC/vmPFC activating primarily during SR and the PCC/PreCun showing increased activation during OR. Using bilinear, deterministic, DCM on DMN core regions and the LIFG as input region, we could demonstrate that contextual modulation of connectivity by SR versus OR is largely inhibitory. Specifically, SR elicits a suppression of information flow from the LIFG to the PCC/PreCun while other-reference is associated with down-regulation of information flow from the LIFG to the rACC/vmPFC, suggesting an inhibitory regulation of self-referential versus other-referential processing in anterior versus posterior DMN subregions.

Inhibitory Control of Information Flow to the DMN

Initially, we had hypothesized that SR and OR would positively modulate the connections leading from the LIFG to the rACC/vmPFC and PCC/PreCun, respectively, and that there might be an additional negative modulation of the within-DMN connections by these 2 conditions. Such a pattern would reflect independent activation and mutual deactivation (Fig. 5A). Instead, Bayesian model averaging – and also the best-fitting model from Bayesian model selection – suggested that self-referential and other-referential processing directly inhibit the transfer of information from the LIFG, a brain structure previously linked to semantic analysis of verbal stimuli (Poldrack et al. 1999; Morin and Michaud 2007; Schott et al. 2013), to the DMN subregions that are preferentially activated during the respective other condition (SR: LIFG → PCC/PreCun; other-reference: LIFG → rACC/vmPFC; Fig. 5C). This pattern corresponds to independent inhibition. While the finding that rACC/vmPFC activity increases during SR whereas PCC/PreCun activity increases during OR is well-established (Qin and Northoff 2011), the observation that this relatively increased activation of anterior versus

posterior DMN structures primarily results from inhibition of information flow to the respective other DMN subregion was unexpected. Inhibitory modulation of information flow was also found within the DMN: OR exerted a negative modulatory influence on the connection from the rACC/vmPFC to the PCC/PreCun (Fig. 5B). The only excitatory modulation of information was observed on the connection from the LIFG to the rACC/vmPFC during SR, and this modulation was not significant after Bonferroni correction.

One parsimonious explanation of the present results would be that task-specific information processing within the DMN might require context-dependent inhibition of information flow into DMN subregions not required for the task at hand. In several previous studies, tasks that are typically believed to engage the DMN have actually yielded reduced deactivations or "negative BOLD responses" in DMN structures rather than absolute activations relative to baseline, a finding that has been reported for emotional picture viewing (Northoff et al. 2007; Grimm et al. 2011), SR (Kelley et al. 2002), Theory of Mind (Schnell et al. 2011) and episodic memory retrieval (Schott et al. 2005). This phenomenon might reflect the inherent difficulty to define a "baseline" of BOLD activity (Gusnard et al. 2001; Morcom and Fletcher 2007). When taking this phenomenon into account, the inhibitory modulation of self-responsive versus other-responsive DMN subregions during the respective opposite experimental condition observed here could be interpreted as an actually rather efficient mechanism of engaging the DMN into specific social cognitive tasks. Previous studies have demonstrated that non-social cognitive tasks associated with DMN deactivation at the same time elicit increased functional and effective connectivity between DMN subregions (Sambataro et al. 2010; Newton et al. 2011; Li et al. 2012). In the present study, however, we employed social cognitive tasks that depend on the function of distinct DMN subregions. We suggest that DMN activity at rest is largely stochastic, with activity shifting spontaneously between subregions, a notion that is supported by the previously reported negative intrinsic effective connectivity of the DMN at rest (Li et al. 2012). At a cognitive level, this may be reflected by an individual's spontaneous switching between – typically self-referential, social, or autobiographical – thoughts ("mind-wandering") (Bado et al. 2014; Kucyi and Davis 2014; Fox et al. 2015). Tasks that require inwardly directed attention, but are triggered externally themselves might in turn require the down-regulation of DMN subregions that are of secondary importance for the respective task.

Our results thus propose an efficient mechanism how the activity of the DMN, which at rest is thought to reflect spontaneous, inwardly directed cognitive processing (Buckner et al. 2008; Fox et al. 2015), can nevertheless be subject to modulation by stimulus-induced activity of brain structures within and outside the DMN (Northoff et al. 2010). An important open question for future research is to determine which brain structures enable the inhibitory control of information flow to the DMN observed here. A recent DCM study has highlighted the role of the salience network in switching between the DMN and the central executive network, and vice versa (Goulden et al. 2014). The salience network responds to both, external stimuli of high importance like pain (Kucyi and Davis 2014), but also to important internal events like errors (Ham et al. 2013) and is therefore a promising candidate network that may mediate the switch between the DMN and networks related to externally directed attention. In the present study, however, the stimuli were comparable in salience, whereas the tasks differed (SR versus OR). While the dorsal anterior cingulate cortex (dACC), a core region of the salience network, has also been implicated in task-switching (Hyafil et al. 2009), the role of the dorsolateral prefrontal cortex (DLPFC), which is also involved in task-switching, requires further investigation. Additionally, the right frontopolar cortex (BA 10) has been associated with switching processes (Yoshida et al. 2010) and, moreover, this region has specifically implicated in modulating the switch between stimulus-dependent and stimulus-independent thoughts (Gilbert et al. 2007). Previous studies have already demonstrated a role for BA 10 in enabling episodic retrieval, a mental operation that engages DMN structures, particularly the PCC/PreCun (Lepage et al. 2000; Schott et al. 2005).

Individual Differences and Potential Clinical Implications

While BMA points to inhibitory modulations of information flow at the entry to the DMN as well as within the DMN, the BMS results further suggest that the averaged model may in fact reflect at least 2 distinct patterns: The scenario suggested by the winning model – a model from Family 1 – is independent of within-DMN inhibitory processes (Fig. 5C), that is, SR and OR as experimental conditions did not modulate the within-DMN connections between rACC/vmPFC and the PCC/PreCun. On the other hand, Family 4 – that is, models with both conditions modulating within-midline connections – also received an increased exceedance probability (Fig. 4B). At the level of single models, one model from this family came out as the second-ranking model in our Bayesian model selection, albeit with a considerably lower exceedance probability than the winning model (EP: 21.67% vs. 67.76%; PEP: 24.04% vs. 55.81%). The most prominent feature of this model is an inhibitory influence of the other-referential condition on both the information flow from the LIFG to the rACC/vmPFC and from the rACC/vmPFC to the PCC/PreCun. Like the winning model, the second-ranking model is therefore also one of primarily inhibitory regulation of information flow to the DMN. Unlike BMA, RFX BMS for DCM aims to account for the possibility that individuals might employ different cognitive strategies to perform a task, resulting in distinct mechanisms of neural processing (Penny et al. 2010). Therefore, the winning and second-ranking model might also represent 2 distinct, albeit related, strategies of task-specific recruitment of the DMN. When adopting this view, task-dependent modulation of within-midline connections might constitute a cognitive strategy adopted by a minority of subjects in the population investigated. We suggest that this model might reflect an intrinsic tendency of these participants to primarily engage in self-referential processing at rest (Gusnard et al. 2001), which in turn needs to be down-regulated at the level of both, input from the left IFG and within-midline connectivity from the rACC/vmPFC to the PCC/PreCun, when the DMN is required for social cognitive processing that is not self-referential.

The observation that, despite the clear dominance of the winning model, two distinct patterns of inhibitory control of information flow to the DMN during social cognitive processing were identified, raises exciting possibilities for clinical research. Dysfunction of the DMN has been suggested to constitute a candidate mechanism underlying large-scale alterations of brain connectivity in neurological and psychiatric disorders, including schizophrenia (Bastos-Leite et al. 2015) and major depressive disorder (MDD) (Li et al. 2013). Given the previously shown altered effective connectivity of the amygdala and

anterior DMN in MDD (Almeida et al. 2011) and the dysregulation of task-positive network connectivity in schizophrenia (Deserno et al. 2012), we suggest that future studies should be aimed at potential contributions of altered information flow to the DMN in psychiatric disorders. This could help to dissect heterogeneous spectrum disorders into biologically informed subgroups (Brodersen et al. 2014; Raman et al. 2016).

Limitations

One important limitation of our study is inherent to the DCM approach, namely the lack of information on brain regions not included in our model. We can therefore not exclude that the information flow from the LIFG to the rACC/vmPFC or to the PCC/PreCun may be indirect, for example via the TPJ, a DMN subregion not included in our model. Along the same line, it is likely that other brain regions, for example, salience network structures (Goulden et al. 2014), also relay information to the DMN, possibly as a function of content or modality. Nevertheless, our results demonstrate the usefulness of DCM in the investigation of regionally specific information transfer to the DMN.

Conclusions

Our results point to the importance of the fact that the DMN is, despite its "task-negative" response profile, strongly connected to "task-positive" brain regions. Information processed by DMN structures, such as self-related concepts, representations of social interactions, or autobiographical memories, is highly multimodal and therefore most likely requires extensive lower-level analysis by brain structures more directly involved in stimulus processing. Our results suggest that the engagement of the DMN in specific tasks is enabled by the inhibitory filtering of such information at the entry to the DMN.

Supplementary Material

Supplementary material can be found at: http://www.cercor.oxfordjournals.org/

Author Contributions

J.S. and B.H.S. designed research, J.S., A.A., A.B., and B.H.S. performed research, J.S., L.D., and B.H.S. analyzed the data, J.S., L.D., H.W., A.R.-K., and B.H.S. wrote the paper.

Funding

This work was funded by the German Research Foundation (DFG) via the Collaborative Research Centre "Neurobiology of Motivated Behavior" (SFB 779, TP A8 and A10) and by the Leibniz Association (LGS "Synaptogenetics").

Notes

We thank MaikeHerbort for help with stimulus preparation and Kerstin Moehring, IlonaWiedenhoeft, and Claus Tempelmann for help with fMRI data acquisition. *Conflict of Interest*: None declared.

References

Almeida JR, Kronhaus DM, Sibille EL, Langenecker SA, Versace A, Labarbara EJ, Phillips ML. 2011. Abnormal left-sided orbitomedial prefrontal cortical-amygdala connectivity during happy and fear face processing: a potential neural mechanism of female MDD. Front Psychiatry. 2:69.

Bado P, Engel A, de Oliveira-Souza R, Bramati IE, Paiva FF, Basilio R, Sato JR, Tovar-Moll F, Moll J. 2014. Functional dissociation of ventral frontal and dorsomedial default mode network components during resting state and emotional autobiographical recall. Hum Brain Mapp. 35:3302–3313.

Bastos-Leite AJ, Ridgway GR, Silveira C, Norton A, Reis S, Friston KJ. 2015. Dysconnectivity within the default mode in first-episode schizophrenia: a stochastic dynamic causal modeling study with functional magnetic resonance imaging. Schizophr Bull. 41:144–153.

Beckmann CF, DeLuca M, Devlin JT, Smith SM. 2005. Investigations into resting-state connectivity using independent component analysis. Philos Trans R Soc Lond B Biol Sci. 360:1001–1013.

Brodersen KH, Deserno L, Schlagenhauf F, Lin Z, Penny WD, Buhmann JM, Stephan KE. 2014. Dissecting psychiatric spectrum disorders by generative embedding. Neuroimage Clin. 4:98–111.

Buckner RL, Andrews-Hanna JR, Schacter DL. 2008. The brain's default network: anatomy, function, and relevance to disease. Ann N Y Acad Sci. 1124:1–38.

Craik FIM, Moroz TM, Moscovitch M, Stuss DT, Winocur G, Tulving E, Kapur S. 1999. IN SEARCH OF THE SELF: A Positron Emission Tomography Study. Psychol Sci. 10:26–34.

Demb JB, Desmond JE, Wagner AD, Vaidya CJ, Glover GH, Gabrieli JD. 1995. Semantic encoding and retrieval in the left inferior prefrontal cortex: a functional MRI study of task difficulty and process specificity. J Neurosci. 15:5870–5878.

Denny BT, Kober H, Wager TD, Ochsner KN. 2012. A meta-analysis of functional neuroimaging studies of self- and other judgments reveals a spatial gradient for mentalizing in medial prefrontal cortex. J Cogn Neurosci. 24:1742–1752.

Deserno L, Sterzer P, Wustenberg T, Heinz A, Schlagenhauf F. 2012. Reduced prefrontal-parietal effective connectivity and working memory deficits in schizophrenia. J Neurosci. 32:12–20.

Di X, Biswal BB. 2014. Identifying the default mode network structure using dynamic causal modeling on resting-state functional magnetic resonance imaging. Neuroimage. 86:53–59.

Fink GR, Markowitsch HJ, Reinkemeier M, Bruckbauer T, Kessler J, Heiss WD. 1996. Cerebral representation of one's own past: neural networks involved in autobiographical memory. J Neurosci. 16:4275–4282.

Fossati P, Hevenor SJ, Graham SJ, Grady C, Keightley ML, Craik F, Mayberg H. 2003. In search of the emotional self: an fMRI study using positive and negative emotional words. Am J Psychiatry. 160:1938–1945.

Fox KC, Spreng RN, Ellamil M, Andrews-Hanna JR, Christoff K. 2015. The wandering brain: Meta-analysis of functional neuroimaging studies of mind-wandering and related spontaneous thought processes. Neuroimage. 111:611–621.

Fox MD, Snyder AZ, Vincent JL, Corbetta M, Van Essen DC, Raichle ME. 2005. The human brain is intrinsically organized into dynamic, anticorrelated functional networks. Proc Natl Acad Sci U S A. 102:9673–9678.

Friston KJ, Harrison L, Penny W. 2003. Dynamic causal modelling. Neuroimage. 19:1273–1302.

Gilbert SJ, Williamson ID, Dumontheil I, Simons JS, Frith CD, Burgess PW. 2007. Distinct regions of medial rostral

prefrontal cortex supporting social and nonsocial functions. Soc Cogn Affect Neurosci. 2:217–226.
Goulden N, Khusnulina A, Davis NJ, Bracewell RM, Bokde AL, McNulty JP, Mullins PG. 2014. The salience network is responsible for switching between the default mode network and the central executive network: replication from DCM. Neuroimage. 99:180–190.
Grimm S, Ernst J, Boesiger P, Schuepbach D, Boeker H, Northoff G. 2011. Reduced negative BOLD responses in the default-mode network and increased self-focus in depression. World J Biol Psychiatry. 12:627–637.
Gruhn D, Smith J. 2008. Characteristics for 200 words rated by young and older adults: age-dependent evaluations of German adjectives (AGE). Behav Res Methods. 40:1088–1097.
Gusnard DA, Akbudak E, Shulman GL, Raichle ME. 2001. Medial prefrontal cortex and self-referential mental activity: relation to a default mode of brain function. Proc Natl Acad Sci U S A. 98:4259–4264.
Ham T, Leff A, de Boissezon X, Joffe A, Sharp DJ. 2013. Cognitive control and the salience network: an investigation of error processing and effective connectivity. J Neurosci. 33: 7091–7098.
Hinrichs H, Scholz M, Tempelmann C, Woldorff MG, Dale AM, Heinze HJ. 2000. Deconvolution of event-related fMRI responses in fast-rate experimental designs: tracking amplitude variations. J Cogn Neurosci. 12(Suppl 2):76–89.
Hyafil A, Summerfield C, Koechlin E. 2009. Two mechanisms for task switching in the prefrontal cortex. J Neurosci. 29:5135–5142.
Jiao Q, Lu G, Zhang Z, Zhong Y, Wang Z, Guo Y, Li K, Ding M, Liu Y. 2011. Granger causal influence predicts BOLD activity levels in the default mode network. Hum Brain Mapp. 32:154–161.
Kelley WM, Macrae CN, Wyland CL, Caglar S, Inati S, Heatherton TF. 2002. Finding the self? An event-related fMRI study. J Cogn Neurosci. 14:785–794.
Kucyi A, Davis KD. 2014. Dynamic functional connectivity of the default mode network tracks daydreaming. Neuroimage. 100:471–480.
Lepage M, Ghaffar O, Nyberg L, Tulving E. 2000. Prefrontal cortex and episodic memory retrieval mode. Proc Natl Acad Sci U S A. 97:506–511.
Li B, Liu L, Friston KJ, Shen H, Wang L, Zeng LL, Hu D. 2013. A treatment-resistant default mode subnetwork in major depression. Biol Psychiatry. 74:48–54.
Li B, Wang X, Yao S, Hu D, Friston K. 2012. Task-Dependent Modulation of Effective Connectivity within the Default Mode Network. Front Psychol. 3:206.
Macrae CN, Moran JM, Heatherton TF, Banfield JF, Kelley WM. 2004. Medial prefrontal activity predicts memory for self. Cereb Cortex. 14:647–654.
Mars RB, Neubert FX, Noonan MP, Sallet J, Toni I, Rushworth MF. 2012. On the relationship between the "default mode network" and the "social brain". Front Hum Neurosci. 6:189.
Martins R, Simard F, Monchi O. 2014. Differences between patterns of brain activity associated with semantics and those linked with phonological processing diminish with age. PLoS One. 9:e99710.
Moran JM, Kelley WM, Heatherton TF. 2013. What Can the Organization of the Brain's Default Mode Network Tell us About Self-Knowledge? Front Hum Neurosci. 7:391.
Moran JM, Macrae CN, Heatherton TF, Wyland CL, Kelley WM. 2006. Neuroanatomical evidence for distinct cognitive and affective components of self. J Cogn Neurosci. 18: 1586–1594.
Morcom AM, Fletcher PC. 2007. Does the brain have a baseline? Why we should be resisting a rest. Neuroimage. 37: 1073–1082.
Morin A, Michaud J. 2007. Self-awareness and the left inferior frontal gyrus: inner speech use during self-related processing. Brain Res Bull. 74:387–396.
Newton AT, Morgan VL, Rogers BP, Gore JC. 2011. Modulation of steady state functional connectivity in the default mode and working memory networks by cognitive load. Hum Brain Mapp. 32:1649–1659.
Northoff G, Qin P, Nakao T. 2010. Rest-stimulus interaction in the brain: a review. Trends Neurosci. 33:277–284.
Northoff G, Walter M, Schulte RF, Beck J, Dydak U, Henning A, Boeker H, Grimm S, Boesiger P. 2007. GABA concentrations in the human anterior cingulate cortex predict negative BOLD responses in fMRI. Nat Neurosci. 10: 1515–1517.
Penny WD, Stephan KE, Daunizeau J, Rosa MJ, Friston KJ, Schofield TM, Leff AP. 2010. Comparing families of dynamic causal models. PLoS Comput Biol. 6:e1000709.
Penny WD, Stephan KE, Mechelli A, Friston KJ. 2004. Comparing dynamic causal models. Neuroimage. 22:1157–1172.
Poldrack RA, Wagner AD, Prull MW, Desmond JE, Glover GH, Gabrieli JD. 1999. Functional specialization for semantic and phonological processing in the left inferior prefrontal cortex. Neuroimage. 10:15–35.
Qin P, Liu Y, Shi J, Wang Y, Duncan N, Gong Q, Weng X, Northoff G. 2012. Dissociation between anterior and posterior cortical regions during self-specificity and familiarity: a combined fMRI-meta-analytic study. Hum Brain Mapp. 33:154–164.
Qin P, Northoff G. 2011. How is our self related to midline regions and the default-mode network? Neuroimage. 57:1221–1233.
Raichle ME, MacLeod AM, Snyder AZ, Powers WJ, Gusnard DA, Shulman GL. 2001. A default mode of brain function. Proc Natl Acad Sci U S A. 98:676–682.
Raman S, Deserno L, Schlagenhauf F, Stephan KE. 2016. A hierarchical model for integrating unsupervised generative embedding and empirical Bayes. J Neurosci Methods. 269:6–20.
Richardson-Klavehn A, Gardiner JM. 1998. Depth-of-processing effects on priming in stem completion: tests of the voluntary-contamination, conceptual-processing, and lexical-processing hypotheses. J Exp Psychol Learn Mem Cogn. 24:593–609.
Rigoux L, Stephan KE, Friston KJ, Daunizeau J. 2014. Bayesian model selection for group studies - revisited. Neuroimage. 84:971–985.
Sajonz B, Kahnt T, Margulies DS, Park SQ, Wittmann A, Stoy M, Strohle A, Heinz A, Northoff G, Bermpohl F. 2010. Delineating self-referential processing from episodic memory retrieval: common and dissociable networks. Neuroimage. 50: 1606–1617.
Salomon R, Levy DR, Malach R. 2014. Deconstructing the default: cortical subdivision of the default mode/intrinsic system during self-related processing. Hum Brain Mapp. 35:1491–1502.
Sambataro F, Murty VP, Callicott JH, Tan HY, Das S, Weinberger DR, Mattay VS. 2010. Age-related alterations in default mode network: impact on working memory performance. Neurobiol Aging. 31:839–852.
Sharaev MG, Zavylova VV, Ushakov VL, Kartashov SI, Velichkovsky BM. 2016. Effective connectivity within the

Default Mode Network: dynamic causal modeling of resting-state fMRI data. Front Hum Neurosci. 10:14.

Schilbach L, Bzdok D, Timmermans B, Fox PT, Laird AR, Vogeley K, Eickhoff SB. 2012. Introspective minds: using ALE meta-analyses to study commonalities in the neural correlates of emotional processing, social & unconstrained cognition. PLoS One. 7:e30920.

Schnell K, Bluschke S, Konradt B, Walter H. 2011. Functional relations of empathy and mentalizing: an fMRI study on the neural basis of cognitive empathy. Neuroimage. 54:1743–1754.

Schott B, Richardson-Klavehn A, Heinze HJ, Duzel E. 2002. Perceptual priming versus explicit memory: dissociable neural correlates at encoding. J Cogn Neurosci. 14:578–592.

Schott BH, Assmann A, Schmierer P, Soch J, Erk S, Garbusow M, Mohnke S, Pohland L, Romanczuk-Seiferth N, Barman A, et al. 2014. Epistatic interaction of genetic depression risk variants in the human subgenual cingulate cortex during memory encoding. Transl Psychiatry. 4:e372.

Schott BH, Henson RN, Richardson-Klavehn A, Becker C, Thoma V, Heinze HJ, Duzel E. 2005. Redefining implicit and explicit memory: the functional neuroanatomy of priming, remembering, and control of retrieval. Proc Natl Acad Sci U S A. 102:1257–1262.

Schott BH, Wustenberg T, Wimber M, Fenker DB, Zierhut KC, Seidenbecher CI, Heinze HJ, Walter H, Duzel E, Richardson-Klavehn A. 2013. The relationship between level of processing and hippocampal-cortical functional connectivity during episodic memory formation in humans. Hum Brain Mapp. 34:407–424.

Spreng RN, Mar RA, Kim AS. 2009. The common neural basis of autobiographical memory, prospection, navigation, theory of mind, and the default mode: a quantitative meta-analysis. J Cogn Neurosci. 21:489–510.

Stephan KE, Kasper L, Harrison LM, Daunizeau J, den Ouden HEM, Breakspear M, Friston KJ. 2008. Nonlinear dynamic causal models for fMRI. NeuroImage. 42:649–662.

Stephan KE, Penny WD, Daunizeau J, Moran RJ, Friston KJ. 2009. Bayesian model selection for group studies. Neuroimage. 46:1004–1017.

Tzourio-Mazoyer N, Landeau B, Papathanassiou D, Crivello F, Etard O, Delcroix N, Mazoyer B, Joliot M. 2002. Automated anatomical labeling of activations in SPM using a macroscopic anatomical parcellation of the MNI MRI single-subject brain. Neuroimage. 15:273–289.

Vo ML, Conrad M, Kuchinke L, Urton K, Hofmann MJ, Jacobs AM. 2009. The Berlin Affective Word List Reloaded (BAWL-R). Behav Res Methods. 41:534–538.

Yoshida W, Funakoshi H, Ishii S. 2010. Hierarchical rule switching in prefrontal cortex. Neuroimage. 50:314–322.

Zhang Y, Fan L, Zhang Y, Wang J, Zhu M, Zhang Y, Yu C, Jiang T. 2014. Connectivity-based parcellation of the human posteromedial cortex. Cereb Cortex. 24:719–727.